Journal of Hazardous Materials 386 (2020) 121655

Contents lists available at ScienceDirect

Journal of Hazardous Materials

journal homepage: www.elsevier.com/locate/jhazmat

Terrestrial-derived soil protein in coastal water: metal sequestration mechanism and ecological function

Qiang Wang[a], Jingyan Chen[b], Shan Chen[a], Lu Qian[a], Bo Yuan[a], Yuan Tian[a], Yazhi Wang[a], Jingchun Liu[a], Chongling Yan[a,b,*], Haoliang Lu[a,**]

[a] Key Laboratory of Ministry of Education for Coastal and Wetland Ecosystems, Xiamen University, Xiamen 361102, China
[b] State Key Laboratory of Marine Environmental Science, Xiamen University, Xiamen 361102, China

GRAPHICAL ABSTRACT

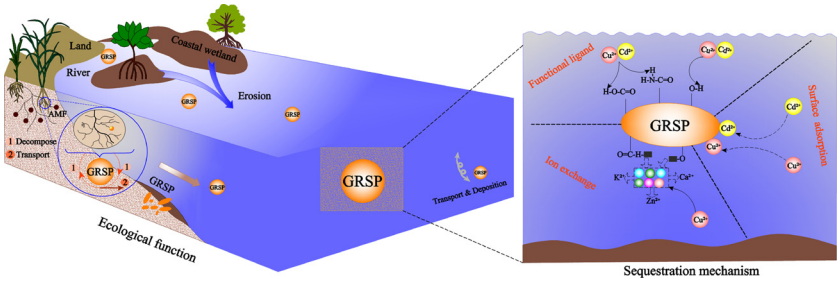

ARTICLE INFO

Editor R Teresa

Keywords:
Glomalin-related soil protein
Arbuscular mycorrhizal fungi
Metal stabilization
Water quality improvement
Estuarine ecosystem

ABSTRACT

Terrestrial fungi, especially arbuscular mycorrhizal (AM) fungi, enhance heavy metal sequestration and promote ecosystem restoration. However, their ecological functions were historically overlooked in discussions regarding water quality. As an AM fungi-derived stable soil protein fraction, glomalin-related soil protein (GRSP) may provide insights into the ecological functions of AM fungi associated with water quality in coastal ecosystems. Here, we first assessed the metal-loading dynamics and ecological functions of GRSP transported into aquatic ecosystems, characterized the composition characteristics, and revealed the mechanisms underlying Cu and Cd sequestration. Combining *in situ* sampling and *in vitro* cultures, we found that the composition characteristics of GRSP were significantly affected by the element and mineral composition of sediments. *In situ*, GRSP-bound Cu and Cd contributed 18.91–22.03% of the total Cu and 2.27–6.37% of the total Cd. Functional group ligands and ion exchange were the principal mechanisms of Cu binding by GRSP, while Cd binding was dominated by functional group ligands. During the *in vitro* experiment, GRSP sequestered large amounts of Cu and Cd and formed stable complexes, while further dialysis only released 25.74 ± 3.85% and 33.53 ± 3.62% of GRSP-bound Cu and Cd, respectively.

1. Introduction

Coastal wetland ecosystems represent the sea–land ecotone and exert control over the biogeochemical processes of metal pollutants at local, regional, and global scales (Bayen, 2012; Fang et al., 2016). Terrestrial materials input to coastal waters provide food for marine

* Corresponding author at: Key Laboratory of Ministry of Education for Coastal and Wetland Ecosystems, Xiamen University, Xiamen 361102, China.
** Corresponding author.
E-mail addresses: ycl@xmu.edu.cn (C. Yan), luhl@xmu.edu.cn (H. Lu).

https://doi.org/10.1016/j.jhazmat.2019.121655
Received 12 August 2019; Received in revised form 9 November 2019; Accepted 9 November 2019
Available online 14 November 2019
0304-3894/

organisms, but excess nutrients lead to eutrophication and increase the susceptibility of coastal waters to ocean acidification and enhance metal bioavailability (Cai et al., 2011; Millero et al., 2009; Xia et al., 2018). Terrestrial materials regulate ecological processes, which will be pivotal in determining how aquatic systems respond to global environmental change (Pace et al., 2004). However, terrestrial fungi and their derivative-mediated ecological functions remain largely unknown.

Arbuscular mycorrhizal (AM) fungi are ubiquitous in soil and form mutualistic symbiotic relationships with the roots of > 80% of terrestrial plants (Smith and Read, 2010; Xie et al., 2014). AM fungal cell walls produce a non-water-soluble substance that persists over long periods (6–42 years) in soil (Rillig et al., 2001), which is named 'glomalin' (Wright and Upadhyaya, 1998), and operationally defined as glomalin-related soil protein (GRSP) (Rillig, 2004). GRSP resistance to decomposition promoted its accumulation in soil during hyphal turnover (Rillig et al., 2001; Zhang J et al., 2017), which contributes to soil C and N sequestration (Lovelock et al., 2004; Rillig et al., 2007). Notably, GRSP can sequester large amounts of heavy metals in terrestrial ecosystems and has been proposed as a mechanism underlying heavy-metal sequestration by AM fungi and their role in soil bioremediation (Gonzalez-Chavez et al., 2004; Cornejo et al., 2008; Vodnik et al., 2008; Malekzadeh et al., 2016). However, the metal sequestration mechanisms of GRSP in both terrestrial and aquatic environments remain unknown. Binding together with organic matter and clay particles, GRSPs can be transported and deposited in coastal wetland as an important nutrient source for marine/aquatic organisms in such environment (Harner et al., 2004; Singh et al., 2017). Transported through rivers and runoff, GRSP can act as a metal carrier to transport large amounts of metals into coastal waters (Chern et al., 2007). In addition, GRSP is transported as a proxy of terrestrial materials and is deposited in coastal waters, providing evidence of its utility as a biological indicator of terrestrial–marine connectivity (Adame et al., 2012; Adame et al., 2010; López-Merino et al., 2015). The links between terrestrial and aquatic nutrient cycles are crucial for aquatic organisms (Pace et al., 2004), but little is known about the ecological roles of GRSP in aquatic ecosystems, including sequestration mechanisms and redistribution patterns of heavy metals.

Our previous research showed that the content of GRSP in mangrove wetlands is significantly higher than that in most terrestrial ecosystems and improves water quality as a metal-binding protein fraction (Wang et al., 2018a; Wang et al., 2019). The use of characterization techniques, such as Fourier transform infrared spectroscopy (FTIR), scanning electron microscopy and energy-dispersive X-ray spectroscopy (SEM-EDX), has helped to better understand GRSP composition (Zhang Z et al., 2017; Wang et al., 2014; Wang et al., 2015). These techniques are also valuable for revealing the sequestration mechanisms of heavy metals (Ozturk et al., 2010; Yue et al., 2015). However, the metal-sequestering mechanisms in both terrestrial and coastal ecosystems, as well as coastal water quality improvement of GRSP, have not been determined. Considering the usefulness of GRSP for metal bioremediation and its significance to land–sea linkages, we carried out the present study to primarily assess the role of GRSP in the binding of heavy metals, namely Cu and Cd. Cu is a common contaminant occurring in coastal environments (Schiff et al., 2004).

As an antifouling coating used on vessel hulls, Cu is recognized as having one of the highest relative mammalian toxicities and to be linked to lung cancer (Schiff et al., 2004). Furthermore, $CuSO_4$ is widely used as an algicide in aquatic systems, which exacerbates water pollution (Fan et al., 2013b). Cd is mainly introduced into water systems from mining and chemical fertilizers and will be enriched in crops and marine organisms and subsequently transferred to the human body through the food web (Li et al., 2012), which causes acute and chronic human diseases resulting from Cd poisoning (Chakraborty et al., 2012). Hence, the need for economical, effective, and safe methods for Cu and Cd removal or stabilization in water systems has directed attention to microbial polymeric substances (Montazer-Rahmati et al., 2011; Bhaskar and Bhosle, 2006). As a stable and ubiquitous terrestrial-fungal-derived substance, GRSP is expected to provide novel methods for water quality improvement and ecosystem restoration.

Here, we ascertained GRSP composition characteristics and its relation with soil environmental parameters (P, K, Ca, Mg, Al, Fe, and Mn content, pH and particle size), as well as its sequestration mechanisms for heavy metals. Based on a combination of *in situ* and *in vitro* studies, and multiple characterization techniques, our study comprised three sections: 1) the characterization of GRSP composition at three geographically separated estuaries and laboratory cultures of indigenous AM fungi; 2) the GRSP contribution to Cu and Cd and sequestration mechanisms of GRSP for Cu and Cd; 3) using GRSP as a novel indicator, our study assessed the metal loading dynamics of terrigenous-derived material into aquatic ecosystems. The overall objective of our study was to investigate the ecological role of terrigenous-derived GRSP and its sequestration mechanisms for heavy metals, which is important for water quality improvements in aquatic ecosystems.

2. Material and methods

2.1. Estuarine ecosystems

2.1.1. Sample collection

Sediment samples were collected from three of China's Estuary ecosystems in autumn 2016; Zhangjiang Estuary (ZJ, 23°55′ N, 117°24′ E), Jiulongjiang Estuary (JL, 24°24′ N, 117°55′ E) and Beilun Estuary (BL, 21°36′ N, 108°12′ E) (Fig. S1). According to the particle size distribution, the JL and ZJ estuarine sediments belong to the mudflat, while the BL sediments were from the sandy beach (Table S1) (Fan et al., 2013a). The level of estuarine heavy metal pollution was as follows: JL > ZJ > BL (Zhang et al., 2014; Liu et al., 2014). We established five field plots (5×5 m^2) spaced at least 50 m apart in each estuary and collected undisturbed sediment samples at 0–10 cm depth from each plot. Each sediment sample was a mixture of five sub-samples collected from each sampling plot. A total of 15 samples were collected. To avoid cross contamination, each sample was collected in a sealed polyethylene bag and stored frozen (−20 °C) before laboratory analysis. After the sediment samples were freeze dried, plant material and stones were removed. Then the dried samples were divided into three parts: one part was used to determine the soil particle size, another was ground using an agate mortar to 0.25 mm for GRSP analysis, and the third was sieved to 0.149 mm to determine trace and macroelements (Wang et al., 2019).

2.1.2. Sediment characteristics

The total content of Fe, Mn, Cu, Cd, and Al were determined in the sediments by pressurizing digestion of 0.1 g of 0.149-mm sieved sediment samples with an acid mixture of concentrated HF, HNO_3, and $HClO_4$ (5/2/1 v/v/v) (Wang et al., 2019). The Fe, Mn, Al, Cu, and Cd content were analyzed by inductively coupled plasma mass spectrometry (Agilent 7700x, Agilent Technologies, USA). P, K, Ca, and Mg were determined by inductively coupled plasma optical emission spectrometer (ICP-OES, Optima 7000 DV, Perkin Elmer, USA). Quality assurance and quality control were assessed using duplicates, method blanks, and the Chinese national certified reference materials (GSD-12) for each set of samples. The grain size composition of the sediments was analyzed using a laser diffraction particle size analyzer (Mastersizer 2000, Malvern, UK), and the median diameter (MD50) was calculated. The sediment pH was measured in a sediment–water suspension (1:5) by a pH meter (PHS-2F).

2.1.3. Extraction and purification of GRSP

GRSP was extracted using the total protein extraction procedure described by Wright and Upadhyaya (1996). GRSP was repeatedly extracted 3–5 times until the supernatant was straw-colored by adding 8 mL of 50 mM sodium citrate solution (pH 8.0) into a 15-mL centrifuge

tube containing 1 g of sediment. For each of the autoclaving cycles (121 °C, 0.1 MPa, 60 min), the supernatant was removed by centrifugation at 8000 × *g* for 10 min (Hettich UNIVERSAL 320 R, Germany) and collected into clean 50-mL centrifuge tubes and stored at 4 °C until purification. Before purification, the extracts were centrifuged at 10,000 × *g* for 10 min to remove all extraneous particles. The gravimetric mass of extracted GRSP, which is referred to as GRSPs, in these samples was collected and measured. Briefly, the above supernatants were precipitated by slowly adding 1 M HCl until the pH of the solution reached 2.0–2.5. The acidified supernatants were incubated in ice for 60 min, followed by centrifugation at 8000 × *g* for 10 min. The precipitate was then re-dissolved in 0.1 M NaOH, dialyzed against deionized water, and freeze-dried.

2.1.4. Chemical analysis

The protein content of the extracted GRSP, which is referred to as GRSPe, was determined spectrophotometrically by the Bradford dye-binding assay using bovine serum albumin as the standard. The total organic C and total N, H, and S content of GRSPs were determined using a Vario EL III CHNOS Elemental Analyzer. The content of GRSPs-bound Cu and Cd were determined using ICP-MS after pressurized acid digestion with a mixture of 4 mL of HNO_3 and 2 mL of H_2O_2 (Gonzalez-Chavez et al., 2004; Wang et al., 2019). The formula for contribution of GRSPs-bound metal (%) was as follows (Wang et al., 2019):

$$\text{Contribution of GRSPs} - \text{bound metal}\ (\%) = \frac{GRSPs\ content \times GRSPs - bound\ metal\ content}{Taltal\ metal\ content} \times 100\%$$

where GRSPs is gravimetric mass of extracted and purified GRSP.

2.1.5. Characteristics of GRSPs

An X-ray diffractometer (XRD, Rigaku Ultima IV) with 2θ radiation source was used to record the X-ray measurements of the GRSPs. Infrared spectra of GRSPs samples (freeze-dried for 48 h) were obtained on a KBr (spectral pure, 120 °C for 12 h) disk with a FTIR (Thermo Scientific Nicolet iS 50) to analyze the functional groups in the GRSPs. To keep it dry, all operations were carried out under infrared light. The matching between functional groups and peak wavenumbers were determined (Johnston and Aochi, 1996; Yuan et al., 2010; Yin et al., 2015). For each peak in the spectrum, the functional group contents were semi-quantified by calculating the absorption peak area (Zhang Z et al., 2017; Wang et al., 2014). SEM-EDX (Zeiss Supra 55, Germany) was used to characterize the surface texture and element composition of the purified GRSPs. We measured the specific surface area of the purified GRSPs using a specific surface area analyzer (ASAP 2020 V4.00, Micromeritics, USA).

2.2. Pot experiment

2.2.1. AM fungal culture

The wet sieving and decantation methods (Gerdemann and Nicolson, 1963) were used to isolate spores of AM fungi from the rhizosphere soils of the mangrove plant *Kandelia obovata* in the JL estuary in October 2016. Then the AM fungal spores were identified based on spore morphology by reference to type descriptions (Smith and Read, 2010). The four dominant AM fungal spores (*Funneliformis geosporum*, *Rhizophagus intraradices*, *Claroideoglomus claroideum*, and *Claroideoglomus etunicatum*) were selected and mixed in the proportion of 6:2:1:1 to prepare the AM fungal inoculum for the pot experiment (Xie et al., 2014).

2.2.2. GRSPs and its characteristics in laboratory culture

Sterile GRSPs-free sand was prepared as per Malekzadeh et al. (2016). The *K. obovata* seedlings were collected from the JL estuary in April 2018. The uniform propagules of *K. obovata* were selected and sterilized with 1% $KMnO_4$ and washed with deionized water. Three *K. obovate* propagules were planted in a cultivating pot (diameter, 20 cm; depth, 35 cm) containing autoclaved sand (2000 g) and were inoculated with the AM fungal inoculum. For the inoculated group (IM), the prepared inoculum (100 g) was thoroughly mixed with the sand, and the same amount of sterilized inoculum was mixed for the non-inoculated group (NM), and then a thin layer of sterilized sand was spread on the top. Each treatment had four duplicates. The plants were grown in a greenhouse under natural light at 32/26 °C in the day/night and were regularly watered with 1/4 Hoagland's nutrient solution without Cu during the growing period. *K. obovata* plants were harvested after 5 months of growth. The root colonization rate was determined by the gridline intersect method under a stereo microscope (Giovannetti and Mosse, 1980). The GRSPs extraction, purification, composition characteristics, and determination of its protein content (GRSPe) were carried out as described above.

2.2.3. In vitro Cu and Cd sequestration by GRSPs

GRSPs was pre-extracted from indigenous AM fungi in a laboratory culture. The 5 mL 400 mg/L Cu ($CuSO_4$) or 400 mg/L Cd ($CdCl_2{\cdot}2.5H_2O$) solutions were introduced into reagent bottles (10 mL) containing 25 mg of GRSPs solids (Gonzalez-Chavez et al., 2004). GRSPs completely precipitated when the metal solution was mixed with GRSPs, and the solution was adjusted to pH 2.5 by adding HCl or NaOH (Table S5). Then the bottles were shaken at room temperature (25 °C) using a mechanical shaker for 30 min to attain the equilibrium. After 30 minutes of standing, the concentration of Cu and Cd in the supernatants were determined by ICP-MS. The control was GRSPs without Cu and Cd. Finally, they were dialyzed against deionized water to: 1) remove possible Cu or Cd that had not been adsorbed by GRSPs; 2) simulate the dynamic change in GRSPs-bound metals in a waterbody through the dialysis process, and all dialyzed samples were freeze-dried. The content of Cu or Cd adsorbed by GRSPs were determined using ICP-MS. The composition characteristics of the freeze-dried GRSPs were also measured by FT-IR, SEM-EDX, and XRD (Zhang Z et al., 2017; Wang et al., 2015) to reveal the sequestration mechanisms of GRSPs for Cu and Cd.

2.3. Statistical analysis

We analyzed the combined data from all plots in the three geographically separated estuaries, as well as the data from laboratory cultures. Data were checked for normal distribution and homogeneity of variances before significance analyses. For the relationship between the GRSPs and its components (protein, C, N, and the C:N ratio), we used a regression analysis. Principal components analysis combined with regression analysis explored the effects of sediment properties on GRSPs variation. One-way ANOVA was performed to test the differences among the three estuarine sites and between IM and NM from laboratory cultures. The statistical analyses were processed using SPSS 22.0 (SPSS, USA). The suitability of all regression models was determined by inspecting residual plots. Correlations and differences were considered significant at $p < 0.05$.

3. Results

3.1. Composition characteristics and metal sequestration of GRSPs

3.1.1. Composition and variation of GRSPs

The chemical composition of C, N, H, and S in the purified GRSPs from the three estuaries are presented in Fig. 1 and Table S2. The percentages of C and S and the C:N ratio within GRSPs in the BL estuary were significantly higher than those of the other two estuaries, but the N content was significantly lower ($p < 0.05$). GRSPs content in sediments was from 15.8 to 48.5 mg g^{-1} sediment. The content of GRSPe determined by the Bradford protein assay was between 2.3 and

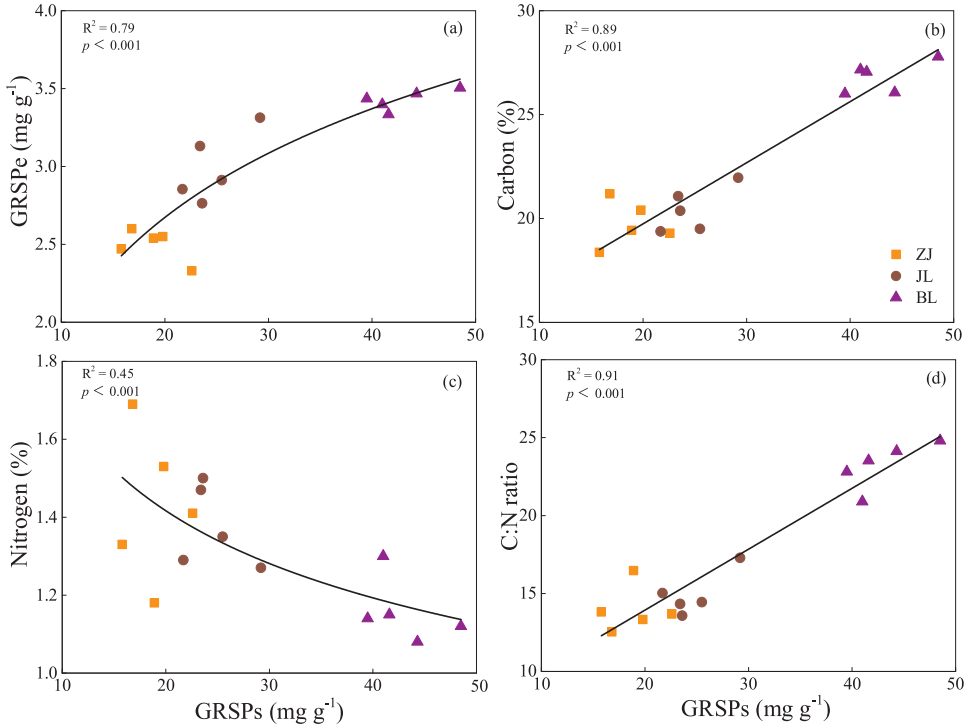

Fig. 1. The content of protein content of glomalin-related soil protein (GRSPe, a), C (b) and N (c), and the C:N ratio (d) of gravimetric mass of extracted GRSP (GRSPs) extracted from sediments from three geographically separated estuaries. ZJ-Zhangjiang Estuary, JL-Jiulongjiang Estuary, and BL-Beilun Estuary.

3.51 mg g^{-1} sediment. The GRSPe content logarithmically increased with increasing GRSPs content, but the proportion of GRSPe decreased as the amount of extracted GRSPs increased (Fig. 1a). Hence, the result indicated a significantly lower proportional contribution of protein to the GRSPs molecule in sediments with higher GRSPs content. The mean C content of GRSPs was 22.33 ± 0.88%, increasing linearly with increasing GRSPs content (Fig. 1b). The N content decreased linearly with increasing GRSPs content in the sediments, and the mean N content was 1.32 ± 0.05% ranging between 1.2 and 1.7% (Fig. 1c). The C:N ratio increased as GRSPs content in the sediments increased (Fig. 1d).

A large number of sediment parameters were significantly correlated with each other; therefore, a principal component analysis was used to test the relationship between sediment characteristics and the GRSP fractions in the top 10 cm of sediments. Based on eigenvalues (eigenvalue > 1), three principal components (PCs) explained 93.37% of the total variance of the total suite of sediment characteristics (Table 1). The PC1 explained 70.12% of the total variation (Table 1). This PC1 was characterized by positive contributions by pH and several parameters associated with soil fertility (elements P, K, Ca, Mn, Fe, and Al), particle size (clay and silt), and negative contributions from sand content and median diameter (MD50). The PC2 explained 14.21% of the total variance and was characterized by strong negative contributions from P, Al, and clay, and positive contributions from Ca (Table 1). The PC3 accounted for 9.04% of the total variation and was characterized by strong positive contribution from Mg (Table 1). GRSPs and GRSPe were significantly negatively correlated with PC1 (Fig. 2a,b).

The functional groups of GRSPs were analyzed using FTIR spectroscopy; the spectra at 4000–500 cm^{-1} are reproduced in Fig. 3. The results of infrared spectroscopy were summarized as follows: the GRSPs showed similar infrared bands in ZJ and JL sediments (mainly silt and clay), whereas in the BL sediments (mainly sand grains), all the absorption peaks were less intense and narrower, especially for composition traits III–VII. Moreover, the FTIR spectra for GRSPs extracted from the three estuarine sediments consisted of a few very broad bands

Table 1
Percentage variation in sediment chemical characteristics explained by the first three eigenvectors using a principal component analysis (PCA), and the contribution of each soil characteristic to each eigenvector.

	Initial eigenvalues			Soil variable	Component matrix		
	Total Total variance explained	% of variance	Cumulative %		PC1 Component matrixes	PC2	PC3
1	8.414	70.120	70.120	pH	0.979	−0.065	0.020
2	1.705	14.210	84.330	Clay	0.800	−0.471	−0.120
3	1.084	9.036	93.366	Silt	0.910	0.319	−0.016
4	0.406	3.381	96.746	Sand	−0.977	0.043	0.071
5	0.139	1.154	97.901	MD50	−0.881	0.053	0.070
6	0.117	0.975	98.876	P	0.859	−0.429	−0.074
7	0.072	0.599	99.475	K	0.974	0.162	0.012
8	0.041	0.344	99.819	Fe	0.974	0.139	−0.119
9	0.017	0.143	99.963	Al	0.767	−0.570	0.042
10	0.004	0.033	99.996	Mn	0.753	0.556	−0.251
11	0.000	0.004	100.000	Ca	0.586	0.687	0.385
12	0.000	0.000	100.000	Mg	0.353	−0.193	0.909

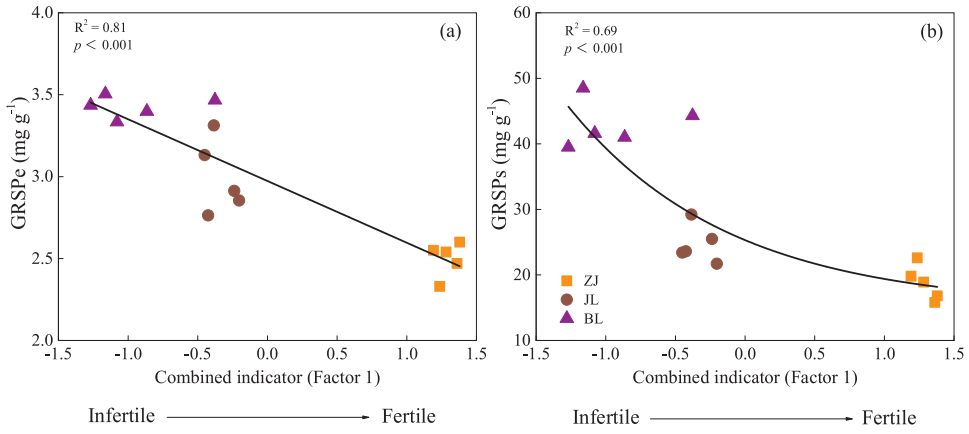

Fig. 2. Relationship between glomalin-related soil protein (GRSP) fractions and combined indicators of soil fertility (Factor 1 derived from a principal component analysis of soil characters, see Table 1).

indicative of complex mixtures (Fig. 3).

SEM micrographs of GRSPs revealed the surface texture and porosity of the samples (Fig. 4). The elements of purified GRSPs from the three estuarine sediments were characterized by SEM-EDX. GRSPs components contained many elements, including C, N, H, O, S, P, Fe, Al, Si, Cl, K, Ca, Na, Mg, Cu, and Zn (Fig. 4 and Table S4), and the content of GRSPs-bound elements, such as C, N, H, and S, showed differences among the estuarine sediments (Table S2; $p < 0.05$). The specific surface area of purified GRSPs was 75.204 $m^2\,g^{-1}$.

3.1.2. Metal sequestration of GRSPs in estuarine sediments

There were significant differences in Cu and Cd content among the three estuaries. The mean Cu content was between 10.43 and 33.52 mg kg^{-1}, with the lowest levels in BL, and the highest by far occurring in JL (Table 2; Fig. S2). A similar pattern was observed for the GRSPs-bound Cu, with 49.02 mg kg^{-1} GRSPs in BL, while it reached 300.09 mg kg^{-1} GRSPs in JL. However, GRSPs-bound Cu contribution to total Cu showed no significant difference among the estuaries ($p > 0.05$; Table 2; Fig. S2).

The mean Cd content was between 0.12 and 0.46 mg kg^{-1}, with JL exhibiting the highest values (3-fold higher Cd than BL and ZJ; Table 2; Fig. S2). Furthermore, GRSPs-bound Cd content was between 0.18 and 0.43 mg kg^{-1}. Its contribution to total Cd reached 6.37% in BL, significantly higher than that of the other estuaries ($p <$ 0.05).

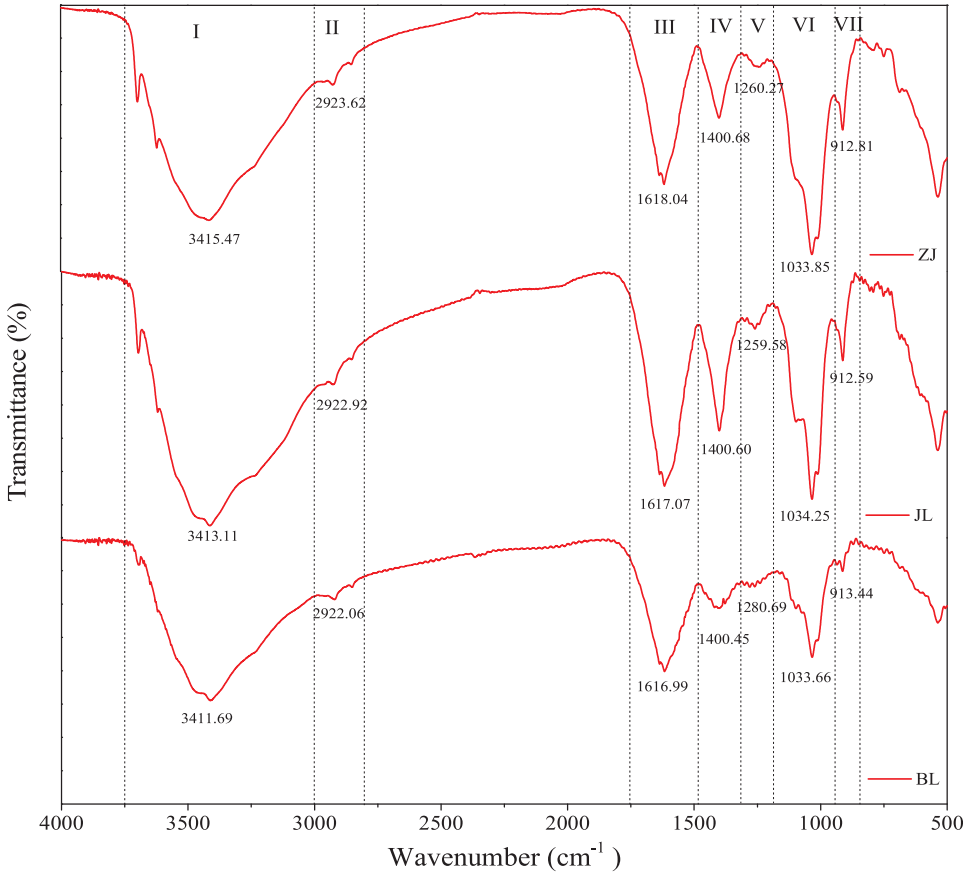

Fig. 3. The functional groups of purified GRSPs were observed by the FTIR spectra in three estuarine sediments. See detailed explanations for the peak in Table S3.

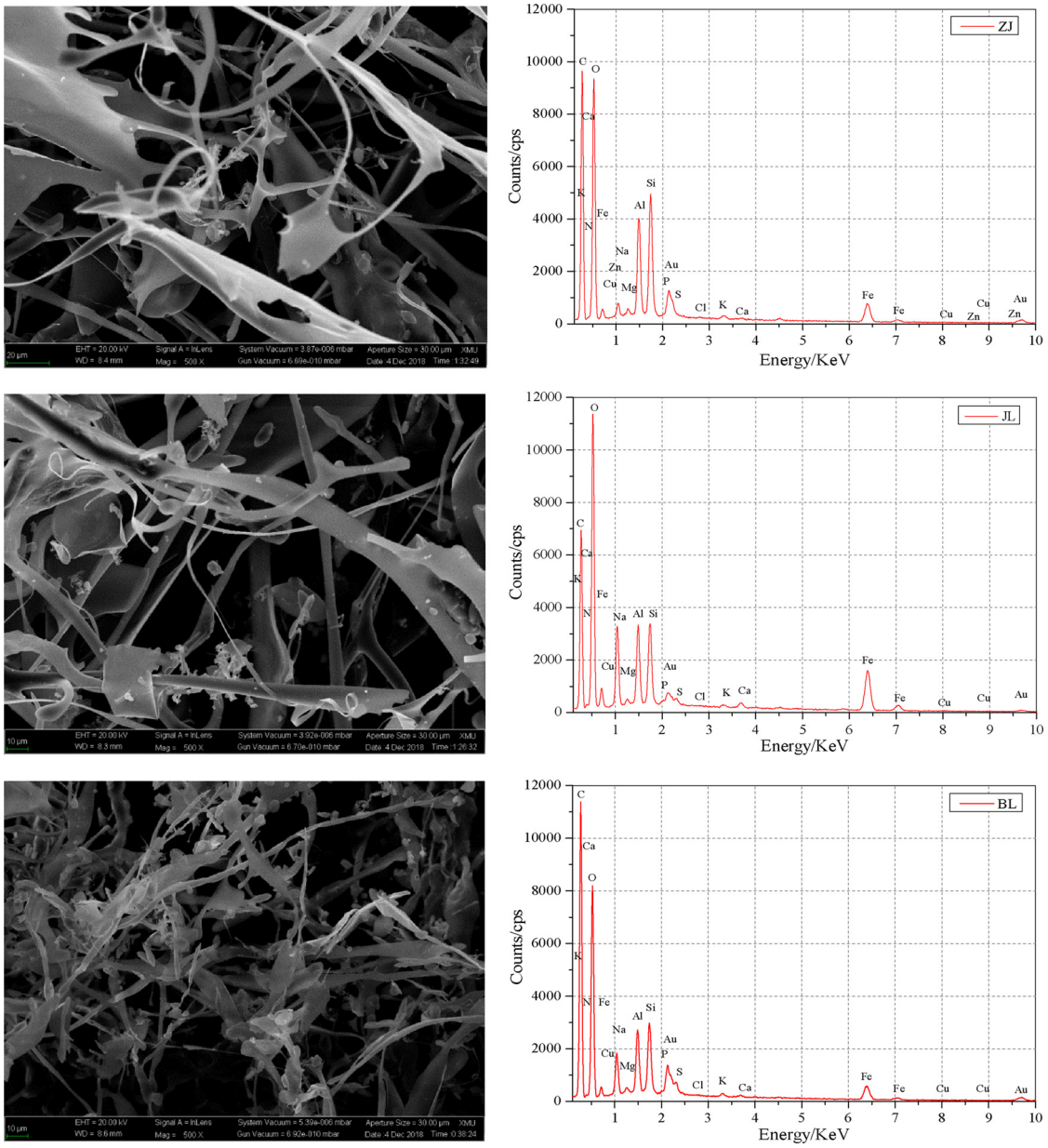

Fig. 4. Ultrastructure and energy spectrum of purified GRSPs from estuarine sediments based on SEM-EDX.

Table 2
GRSPs-bound Cu and Cd (mg kg^{-1} GRSPs) and their contributions (%) to the total Cu and Cd content (mg kg^{-1} sediment) in sediments from three estuaries.

Sampling sites	Total metal (mg kg^{-1} sediment)		GRSPs-bound metal (mg kg^{-1} GRSPs)		Contribution of GRSPs-bound metal (%)	
	Cu	Cd	Cu	Cd	Cu	Cd
ZJ	16.22 ± 0.48b	0.16 ± 0.01b	163.08 ± 7.14b	0.23 ± 0.01 b	18.91 ± 1.32 a	2.72 ± 0.26 b
JL	33.52 ± 0.31a	0.46 ± 0.02a	300.09 ± 16.9a	0.43 ± 0.02 a	22.03 ± 1.51 a	2.27 ± 0.14 b
BL	10.43 ± 0.47c	0.12 ± 0.04b	49.02 ± 5.82 c	0.18 ± 0.02 b	20.22 ± 2.29 a	6.37 ± 0.54 a
ANOVA						
Mean	20.06	0.25	170.73	0.28	20.38	3.79
F-value	788.32	244.45	127.35	69.18	0.80	40.22
SE	2.63	0.04	28.07	0.03	1.00	0.53
p	< 0.001	< 0.001	< 0.001	< 0.001	> 0.05	M0.001

Note: Different letters represent significant differences between sites ($p < 0.05$).

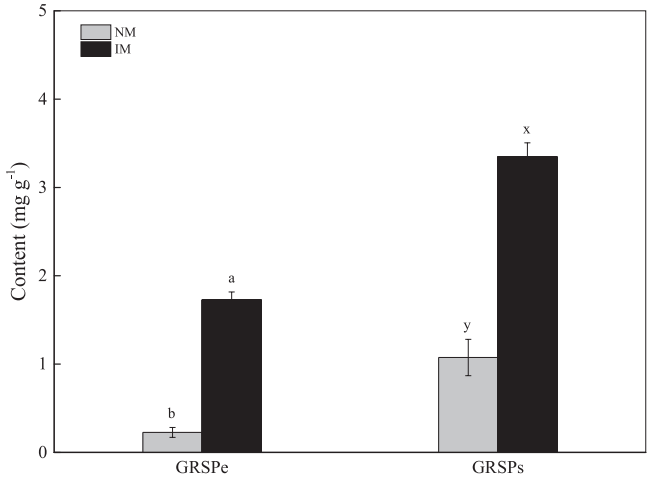

Fig. 5. Contents of GRSPs and GRSPe of the treatments inoculated with arbuscular mycorrhizal (AM) fungi (IM) or non-inoculated (NM).

3.2. *In situ* and *in vivo* comparison of GRSPs

3.2.1. *In vivo* AM fungi-derived GRSPs

All plant roots were colonized by the AM fungi in IM. Intracellular hyphae and arbuscules were the dominant structures, and the root colonization rate was 46.18 ± 2.33% (40.63–51.49%) in IM. Conversely, no mycorrhizal structures were observed in NM. The mean GRSPs was 3.35 ± 0.16 and 1.08 ± 0.21 mg g^{-1} in IM and NM, respectively (Fig. 5). The mean GRSPe content in IM and NM was 1.73 ± 0.09 and 0.23 ± 0.06 mg g^{-1}, respectively. The content of GRSPs and GRSPe were significantly higher in IM than in NM ($p < 0.05$), and the proportion of GRSPe that was detected by the protein assay was 51.96 ± 4.02% and 20.48 ± 1.66% in IM and NM, respectively.

3.2.2. Composition characteristics of GRSPs

The proportion of GRSPe against GRSPs was significantly higher in laboratory cultures than in JL sediments ($p < 0.05$). The absorption peak area of the infrared spectrum was measured to evaluate structural differences in GRSPs from the laboratory cultures (*In vivo*) and JL sediments (*In situ*). Similar infrared bands were observed, whereas the variation in relative absorption peak area between laboratory cultures and JL sediments for different composition traits differed (Fig. 6). The relative content of composition traits I (O–H, N–H, and C–H stretching) and VII (O–H bending and asymmetric ester O–P–O stretching) were higher in JL sediments than those in laboratory cultures, while the

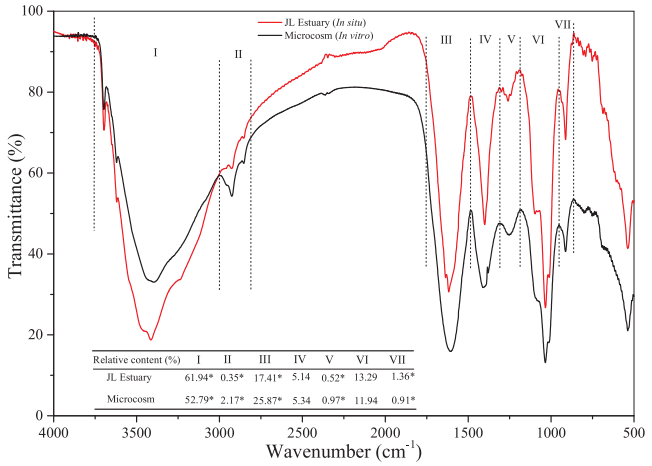

Fig. 6. FTIR spectra of purified GRSPs produced from *in vivo* and *in situ*. Asterisk (*) represents significant differences ($p < 0.05$).

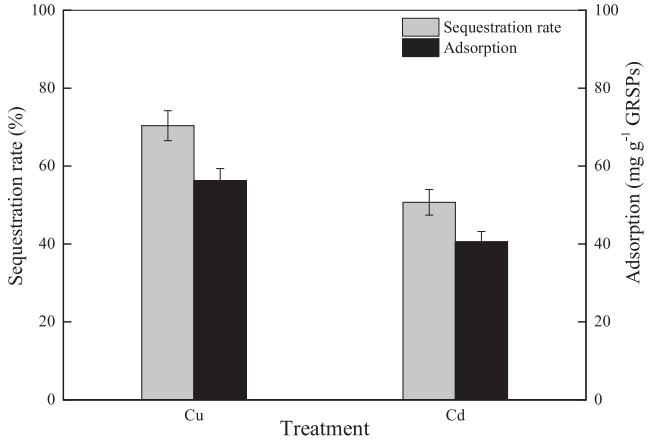

Fig. 7. *In vitro* sequestration rates (%) of Cu and Cd and adsorption of GRSPs (mg g^{-1} GRSPs) from laboratory cultures.

relative content of composition traits II (aliphatic C–H stretching), III (C═O and −COO stretching), and V (C–O and C–N stretching, and O–H bending) were higher in laboratory cultures (Fig. 6, Table S3).

3.3. Heavy-metal sequestration mechanisms of GRSPs

3.3.1. *In vitro* Cu and Cd sequestration capacity of GRSPs

GRSPs from laboratory cultures removed Cu or Cd from aqueous solutions. GRSPs precipitated immediately at pH 2.5. The supernatant contained an average of 5.28 ± 0.30% Cu (4.86–5.86%) and 23.81 ± 0.93% Cd (22.53–25.62%), indicating that most of the Cu and Cd were adsorbed by GRSPs, and its ability to remove Cu is significantly higher than its ability to remove Cd ($p < 0.05$). After dialysis, the mean GRSPs-sequestered Cu and Cd was 56.28 ± 3.08 and 40.56 ± 2.64 mg g^{-1} GRSPs, respectively, representing 70.35 ± 3.85% of the total Cu and 50.70 ± 3.30% of the total Cd added (Fig. 7). Notably, by simulating the dynamics of GRSPs-bound metals by the dialysis method, we found that 25.74 ± 3.85% and 33.53 ± 3.62% of GRSPs-bound Cu and Cd were released into the waterbody again, respectively.

3.3.2. Cu and Cd sequestration mechanisms of GRSPs

The components of GRSPs that were responsible for Cu and Cd sequestration, and the corresponding binding capacity was determined based on FTIR, SEM-EDX, and XRD analyses (Figs. 8 and 9, S4). The changes in peak frequency of the FTIR spectra of the original and metal-loaded GRSPs suggested that active functional groups, particularly C–O, C = O, C–N, O–H, and –COO$^-$, were involved in Cu and Cd sequestration (Fig. 8, Table S3). Notably, functional group V (C–O stretching and O–H bending of − COOH; C–N stretching associated with secondary amides of proteins) disappeared when GRSPs adsorbed Cu or Cd. Furthermore, the spectra of Cu- and Cd-sequestrated GRSPs were significantly different, particularly for functional group IV (symmetric –COO$^-$ stretching in carboxylic acid salts; C = O symmetric stretching of –COO$^-$ groups).

The metal-binding capacities of GRSPs were assessed using SEM-EDX, and the image shows the microscopic photographs and energy spectra for the original and metal-loaded GRSPs (Fig. 9). By optimizing the pH to pH 2.5, the micrograph of freeze-dried GRSPs showed an irregular block-shaped structure. In contrast to the original energy spectra of GRSPs, the Zn and Na peaks disappeared, and the K and Ca peak intensities significantly decreased as Cu was adsorbed. However, the sorption of other elements were not disturbed by the presence of Cd (Figs. 9 and 10; Table S4). Furthermore, GRSPs may promote surface adsorption of Cu and Cd owing to its glue-like and non-water-soluble properties and high specific surface area (Fig. 10).

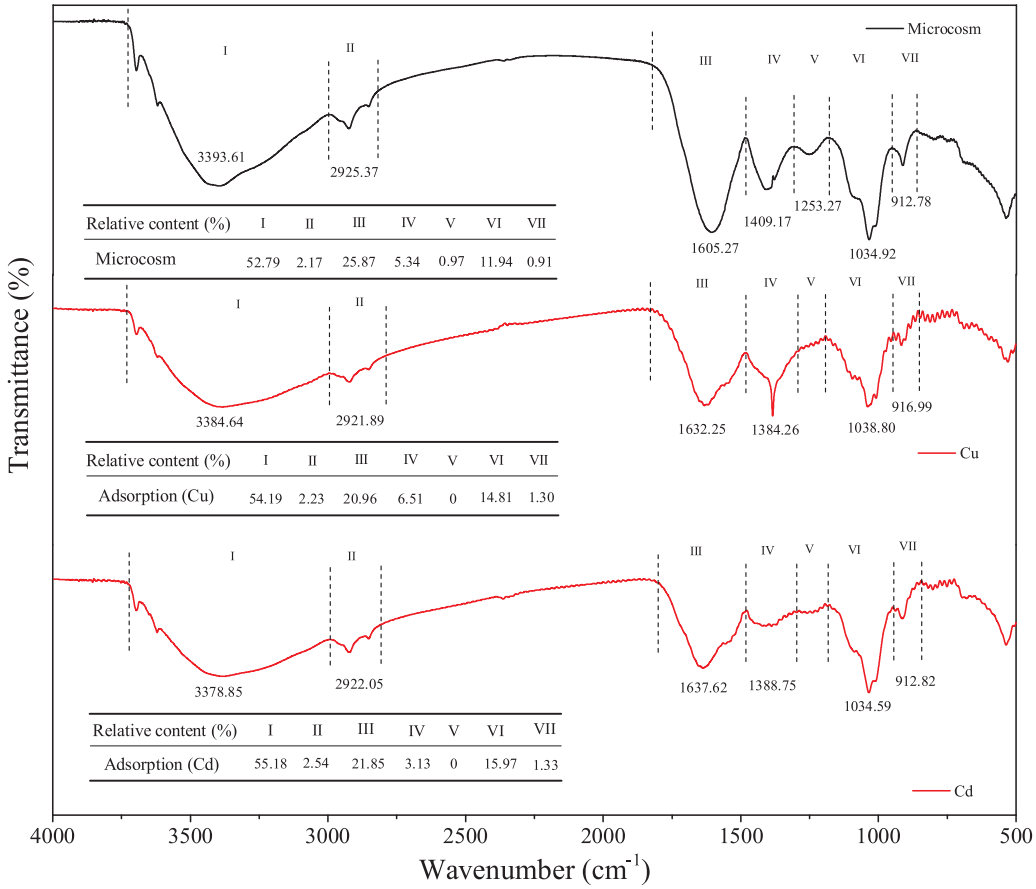

Fig. 8. FTIR spectra of purified GRSPs and GRSPs-bound Cu and Cd produced from laboratory cultures of indigenous arbuscular mycorrhizal (AM) fungi.

4. Discussion

4.1. Composition characteristics of GRSPs

GRSPs has been quantified in diverse soil types, and results indicated that a variety of environmental factors, including soil characteristics, land use, climate conditions, and vegetation type, can affect the GRSPs content and composition (Schindler et al., 2007; Zhang et al., 2015; Kumar et al., 2018). However, few studies have focused on the GRSPs content and composition and their role in coastal wetlands.

The results of the present study suggested that the amount of GRSP fractions extracted from the three estuarine sediments agreed with the range of GRSPs and its protein content previously reported for mineral and tropical soils (Schindler et al., 2007; Kumar et al., 2018; Singh et al., 2016). Coastal wetland ecosystems, as the link between terrestrial and marine systems, buried large amounts of C (Bouillon, 2011). Thus, a relatively high amount of GRSP fractions in the sediments were expected since previous research has shown that GRSP fractions are significantly positively correlated with total organic C content in sediments (Wang et al., 2018a; Wang et al., 2018b). Studies have shown that GRSPe accounts for up to 27% of the soil organic C (Lovelock et al., 2004; Zhang et al., 2015). This is consistent with the contribution of GRSPe to SOC (8.9–23.5%) observed in our study. Our results show that GRSPs content was significantly positively correlated with GRSPe and C, and the C:N ratio but was negatively correlated with N content, indicating that chemical composition of GRSPs varied with changing GRSPs content (Lovelock et al., 2004; Schindler et al., 2007). GRSPs and GRSPe content were significantly negatively correlated with soil fertility (Table 1; Fig. 2), which is consistent with that reported previously from a tropical lowland rainforest (Lovelock et al., 2004). The sensitivity of GRSP to soil characteristics is likely to be an important reason for component differences (Zhang Z et al., 2017; Schindler et al., 2007).

Studies have reported that the composition characteristics of GRSPs primarily contain groups that represent the stretching of O–H, N–H, C–H, C = O, –COO^-, C–O, C–N, and Si–O–Si, and bending of C–H and O–H (Figs. 3 and 6); soil pH, salinity, and soil type are important factors affecting the peak intensity of GRSPs components (Zhang Z et al., 2017; Wang et al., 2015; Schindler et al., 2007). However, the differences between GRSPs composition characteristics in different estuarine sediments have not been determined. Our results indicated that there were differences in the composition characteristics of the GRSPs from the three estuarine sediments that we tested, especially between the BL estuary and the ZJ and JL estuaries (Fig. 3). For example, the infrared spectral absorption peaks of GRSPs were less intense and narrower for composition traits III–VII in the BL sediments (Fig. 3). Previous studies have shown that the basement type of ZJ and JL is mudflats dominated by silt and clay, while BL is a beach dominated by sand (Ding et al., 2009). The particle size distribution of sediments in these estuaries also provided evidence to support this characterization (Table S1). Moreover, the infrared spectra indicated that the purified GRSPs contained functional groups associated with macromolecular substances. Peaks I and II were associated with hydrocarbons; III–V were associated with proteins; VI was associated with polysaccharides; and VII was associated with nucleic acids (Fig. 3; Table S3) (Yin et al., 2015). These results were consistent with those of recent studies that reported GRSPs to be a mixture of many compounds (Zhang Z et al., 2017; Gillespie et al., 2011). Combined with SEM-EDX, our results indicated that GRSPs was a complex mixture and contained many elements, such as C, N, H, O, S, Cl, P, K, Ca, Mg, Na, Zn, Cu, Fe, Si, and Al in the sediments (Fig. 4; Fig. S3).

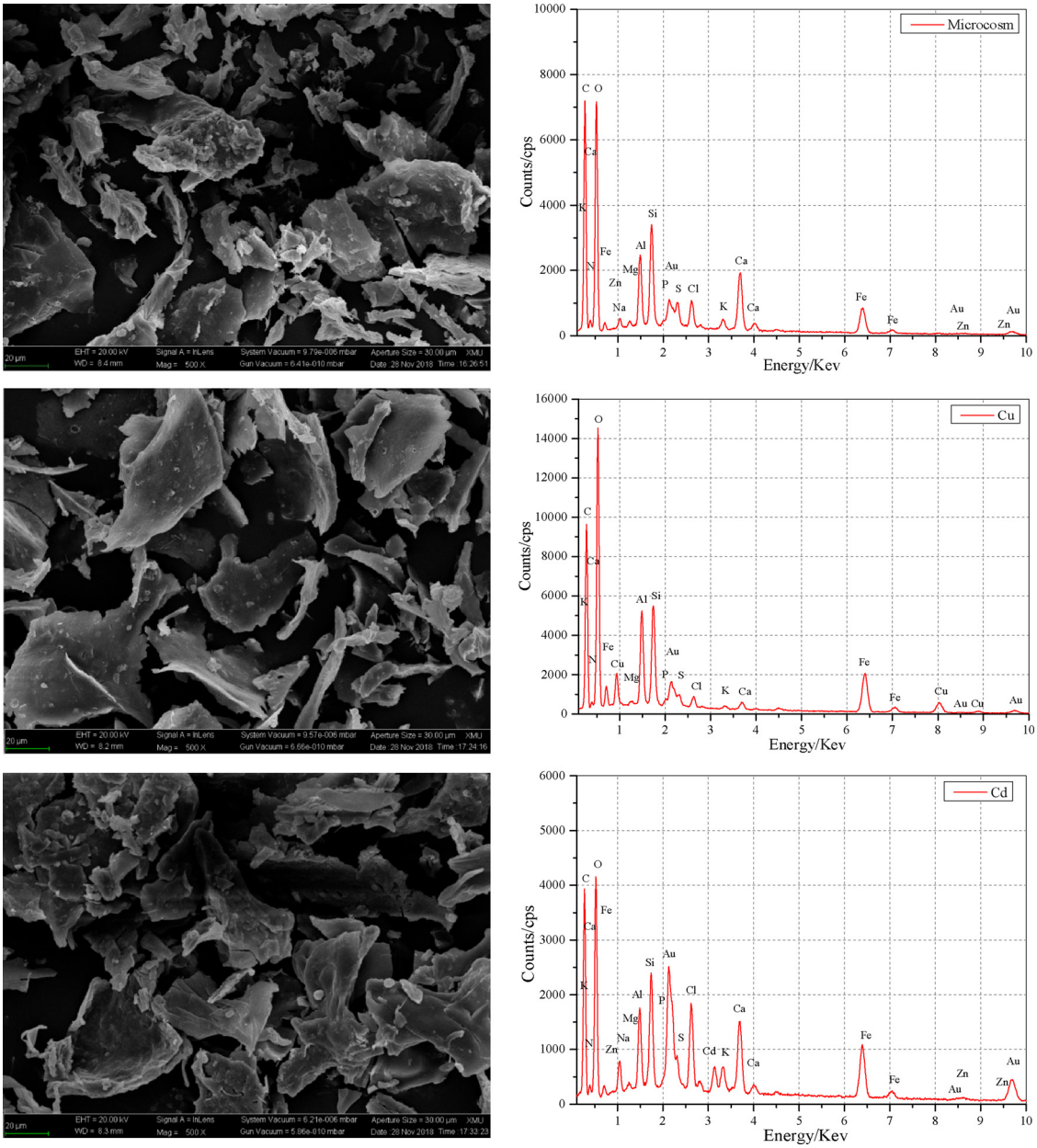

Fig. 9. Ultrastructure and energy spectrum of *in vitro* purified GRSPs and GRSPs-bound Cu/Cd at pH 2.5 based on SEM-EDX.

4.2. GRSPs sequestered heavy metals in aquatic ecosystem

In the three estuaries, the content of GRSPs-bound Cu and Cd were 49.02–300.09 mg kg^{-1} and 0.18–0.43 mg kg^{-1}, which contributed 18.91–22.03% and 2.27–6.37% to the total Cu and Cd content in the sediments, respectively (Table 2; Fig. S2). These results indicated that GRSPs could efficiently sequester Cu and Cd and that it possessed a higher capacity for binding Cu in coastal wetlands. The significant difference in the metal-sequestration capacity of GRSPs in different estuarine zones could be explained by the total metal content of the sediments since GRSPs-bound Cu and Cd were positively associated with total-metal content (Fig. S2). Alternatively, this may be due to the differences in the absorption peak intensity of functional groups (Fig. 3), even though large amounts of extraneous proteins were not present because the extraction of GRSPs was conducted at high temperature (121 °C), which denatured many of the proteins (Driver et al., 2005).

Recent studies have indicated that GRSPs can bind and sequester large amounts of heavy metals, such as Cu, Cd, Pb, and Zn (Gonzalez-Chavez et al., 2004; Cornejo et al., 2008; Chern et al., 2007). However, the heavy-metal binding mechanisms of GRSPs remain largely unknown. The FTIR spectra of the original and metal-loaded GRSPs identified the functional groups in GRSPs responsible for Cu and Cd sorption (Fig. 8, Table S5). We found that, compared with the original GRSPs, the absorption intensity of infrared absorption peaks III (amide I, C = O and $-COO^-$ stretches), IV (amide II, $-COO^-$ and C = O stretching), V (amide III, C–O, and C–N stretching, and O–H bending), VI (C–O and Si–O–Si stretches), and VII (O–H bending) of the metal-loaded GRSP were weakened and narrower (Fig. 8, Table S5). Previous studies showed that functional groups III–V are associated with proteins, while bands at VI and VII are associated with polysaccharides and nucleic acids, respectively (Yuan et al., 2010; Yin et al., 2015). This indicates that GRSPs-bound heavy metals were mainly associated with proteins, polysaccharides, and nucleic acids. Furthermore, previous studies have demonstrated that the carbonyl (C═O), hydroxyl (O–H), amide (−CO−NH), and carboxyl (−COO−) functional groups show very

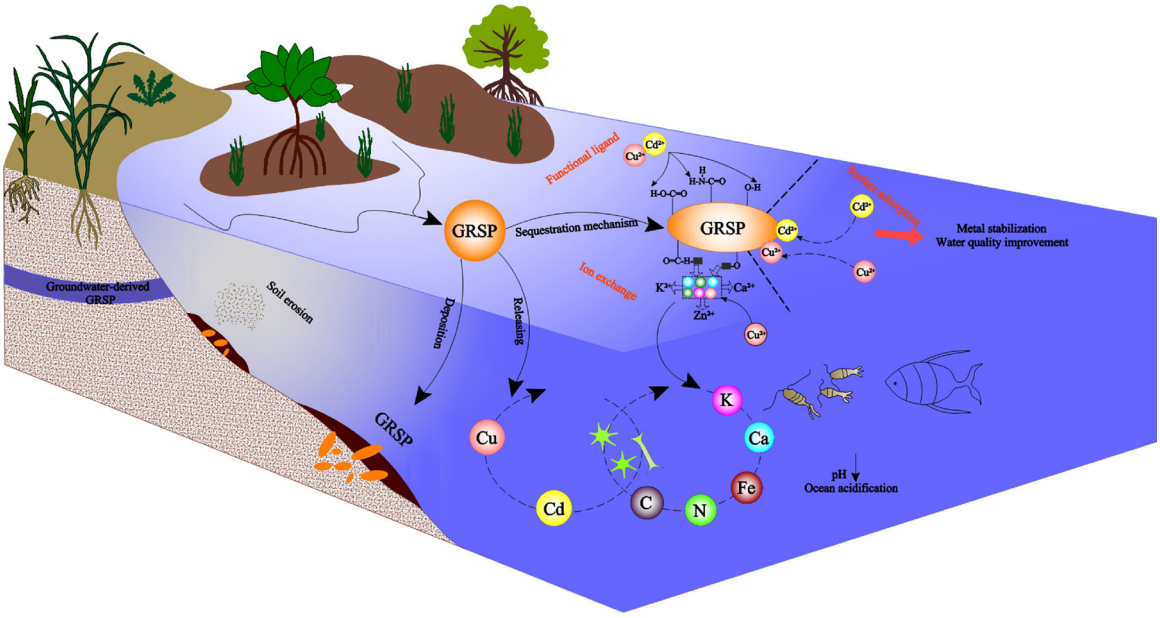

Fig. 10. GRSP fraction promoted water quality improvement and bioremediation of heavy metals in the aquatic environment. It enters coastal water via rivers through erosion and sequestered heavy metals primarily through the process of ion exchange and functional group ligands.

high coordination with heavy metals (Yue et al., 2015; Sheng et al., 2010).

The results of the present study showed that Cu- and Cd-sequestration rates by purified GRSPs were significantly higher than GRSPs extracted from the estuarine sediments (Fig. 7). Notably, the GRSPs in the laboratory cultures or sediments also adsorbed other elements, such as Fe, Si, Al, K, Ca, Na, Mg, and Zn (Fig. 4; Table. S4). Previous studies have shown that the procedures used for the extraction and purification of GRSPs may release other cations that may occupy binding sites, such as Ca, Mg, and K (Gonzalez-Chavez et al., 2004). However, there remains a lack of evidence regarding ion exchange as an important mechanism for metal sequestration by GRSPs. The energy spectra of the original and metal-loaded GRSPs were used to identify the ion exchange mechanism responsible for Cu and Cd sequestration by SEM-EDX analysis. These apparent Cu and Cd spectra peaks were observed when GRSPs was mixed with Cu or Cd solution, which further confirmed that GRSPs could sequester a large amount of heavy metals in the aquatic environment. The most remarkable observation was that the energy spectra peaks of Zn and Na disappeared, and the energy spectra peaks of K and Ca were significantly weaker when GRSPs bound Cu, but there was no significant change in GRSPs-bound Cd. Thus, ion exchange was the principal mechanism for Cu sequestration but not for Cd, suggesting that GRSPs possessed a higher binding capacity for Cu. In conclusion, functional group ligands and ion exchange were the principal mechanisms for Cu sequestration, which further confirmed mechanisms speculated by previous studies (Gonzalez-Chavez et al., 2004).

4.3. Land–sea linkage: water quality improvement

As a microorganism unique to terrestrial ecosystems, AM fungi can form mycorrhizal symbioses with more than 80 % of all plant species and promote ecosystem restoration (Smith and Read, 2010). Although AM fungi can colonize most terrestrial plant roots, the ability of AM fungi to colonize plant roots is limited by salinity and anoxic conditions, and AM fungi colonization of mangrove plant roots remains unclear (Xie et al., 2014; Wang et al., 2010). In the present study, we found that inoculation with indigenous AM fungi selected from mangrove sediments allowed the successful colonization of the roots of the mangrove plant *K. obovata*, which is consistent with our previous research (Xie et al., 2014). Compared to non-AM fungi, GRSPs and GRSPe were significantly higher after inoculation with AM fungi (Fig. 5), indicating that AM fungi was an important driver and source of GRSPs. These results provide evidence that supports previous studies regarding GRSPs being a component of AM fungal spores and mycelial cell walls (Driver et al., 2005; Gao et al., 2017). Therefore, GRSPs could be used as a proxy for the ecological functions of terrestrial fungi in coastal water since it has a known origin, high stability, and is easily measured. Thus, its dynamics in aquatic environments can be used as an indicator of land–sea linkages (Harner et al., 2004; Adame et al., 2012; López-Merino et al., 2015) (Fig. 10).

GRSPs is an important component of soil organic matter, and thus serves as a nutrient source for aquatic organisms (Harner et al., 2004). However, other ecological functions (metal sequestration) and dynamics (metal release) of GRSPs in aquatic environments remain unknown (Fig. 10). We analyzed the metal-sequestration capacity of GRSPs *in situ* and *in vitro* and simulated dynamics through a dialysis treatment (adsorption and desorption) of GRSPs-bound metals in a waterbody as a novel indicator of terrestrial-derived material. The most remarkable observation was that 70.35 ± 3.85% and 50.70 ± 3.30% of the total added Cu and Cd, respectively, were retained following the dialysis treatment (Fig. 7), which suggested that GRSPs bound heavy metals and formed strong stable complexes. Furthermore, the specific surface area of purified GRSPs was 75.204 $m^2 g^{-1}$, indicating that it provided pores and internal surface for metal adsorption. Thus, as GRSPs-bound heavy metals are transferred into the coastal water through soil erosion, the metal sequestration by GRSPs was far greater than metal release, which plays an important role in water quality improvement.

Furthermore, we have found that GRSPs defined by the current extraction procedure was a novel natural bioflocculant and had a higher flocculating activity at lower pH (Table S5). FTIR analysis demonstrated the presence of hydroxyl, amide, carboxyl, and amine groups in GRSPs. These groups represent important functional groups contributing to bioflocculation based on microbial polymeric substance analysis (Yuan et al., 2010; Sun et al., 2015). Our study provides insights into the metal-sequestration mechanisms of GRSPs and the dynamics of GRSPs-bound metals in coastal water and provides a complimentary tool for water quality improvement (Fig. 10). However, the relationship between the constituents and structure of GRSPs with its flocculation capacity and the effects on water quality improvement

should be further explored in future studies.

5. Conclusions

AM-fungi-derived GRSPs was a mixture containing protein and polysaccharides and was widely distributed in coastal zones contributing to water quality. GRSPs sequestered large amounts of Cu and Cd in coastal wetlands. Functional group ligand complexes and ion exchange were predominant binding mechanisms for Cu and Cd with GRSPs. As a novel indicator of terrestrial material, GRSPs sequestered heavy metals and formed stable complexes in waterbodies, enhancing heavy-metal stabilization and promoting water quality. Our findings provide evidence pertaining to the role of GRSPs in Cu and Cd sequestration and new insights into the ecological restoration of heavy metals by AM fungi in aquatic environments.

Author contribution

Qiang Wang: Conceptualization, Data curation, Formal analysis, Investigation, Methodology, Software, Writing - original draft and review & editing. Jingyan Chen: Writing - original draft and review & editing, Investigation. Shan Chen, Lu Qian, Bo Yuan, Yuan Tian, and Yazhi Wang: Visualization, Investigation. Chongling Yan, Haoliang Lu, and Jingchun Liu: Funding acquisition, Project administration, Resources, Supervision and Validation.

Declaration of Competing Interest

None.

Acknowledgments

This work was kindly supported by National Important Scientific Research Programme of China (2018YFC1406603, 2016YFA0601402), and National Natural Science Foundation of China (31870483, 31530008).

References

Adame, M.F., Neil, D., Wright, S.F., Lovelock, C.E., 2010. Sedimentation within and among mangrove forests along a gradient of geomorphological settings. Estuar. Coast. Shelf Sci. 86, 21–30. https://doi.org/10.1016/j.ecss.2009.10.013.

Adame, M.F., Wright, S.F., Grinham, A., Lobb, K., Reymond, C.E., Lovelock, C.E., 2012. Terrestrial–marine connectivity: patterns of terrestrial soil carbon deposition in coastal sediments determined by analysis of glomalin related soil protein. Limnol. Oceanogr. 57, 1492–1502. https://doi.org/10.4319/lo.2012.57.5.1492.

Bayen, S., 2012. Occurrence, bioavailability and toxic effects of trace metals and organic contaminants in mangrove ecosystems: a review. Environ. Int. 48, 84–101. https://doi.org/10.1016/j.envint.2012.07.008.

Bhaskar, P., Bhosle, N.B., 2006. Bacterial extracellular polymeric substance (EPS): a carrier of heavy metals in the marine food-chain. Environ. Int. 32, 191–198. https://doi.org/10.1016/j.envint.2005.08.010.

Bouillon, S., 2011. Carbon cycle: storage beneath mangroves. Nat. Geosci. 4, 282.

Cai, W.-J., Hu, X., Huang, W.-J., Murrell, M.C., Lehrter, J.C., Lohrenz, S.E., Chou, W.-C., Zhai, W., Hollibaugh, J.T., Wang, Y., 2011. Acidification of subsurface coastal waters enhanced by eutrophication. Nat. Geosci. 4, 766. https://doi.org/10.1038/NGEO1297.

Chakraborty, P., Babu, P.R., Sarma, V., 2012. A study of lead and cadmium speciation in some estuarine and coastal sediments. Chem. Geol. 294, 217–225. https://doi.org/10.1016/j.chemgeo.2011.11.026.

Chern, E.C., Tsai, D.W., Ogunseitan, O.A., 2007. Deposition of glomalin-related soil protein and sequestered toxic metals into watersheds. Environ. Sci. Technol. 41, 3566–3572. https://doi.org/10.1021/es0628598.

Cornejo, P., Meier, S., Borie, G., Rillig, M.C., Borie, F., 2008. Glomalin-related soil protein in a Mediterranean ecosystem affected by a copper smelter and its contribution to Cu and Zn sequestration. Sci. Total Environ. 406, 154–160. https://doi.org/10.1016/j.scitotenv.2008.07.045.

Ding, Z.H., Liu, J.L., Li, L.Q., Lin, H.N., Wu, H., Hu, Z.Z., 2009. Distribution and speciation of mercury in surficial sediments from main mangrove wetlands in China. Mar. Pollut. Bull. 58, 1319–1325. https://doi.org/10.1016/j.marpolbul.2009.04.029.

Driver, J.D., Holben, W.E., Rillig, M.C., 2005. Characterization of glomalin as a hyphal wall component of arbuscular mycorrhizal fungi. Soil Biol. Biochem. 37, 101–106. https://doi.org/10.1016/j.soilbio.2004.06.011.

Fan, D.D., Wang, Y., Liu, M., 2013a. Classifications, sedimentary features and facies associations of tidal flats. J. Palaeogeog. 2, 66–80. https://doi.org/10.3724/SP.J.1261.2013.00018.

Fan, J., Ho, L., Hobson, P., Brookes, J., 2013b. Evaluating the effectiveness of copper sulphate, chlorine, potassium permanganate, hydrogen peroxide and ozone on cyanobacterial cell integrity. Water Res. 47, 5153–5164. https://doi.org/10.1016/j.watres.2013.05.057.

Fang, H., Huang, L., Wang, J.Y., He, G., Reible, D., 2016. Environmental assessment of heavy metal transport and transformation in the Hangzhou Bay, China. J. Hazard. Mater. 302, 447–457. https://doi.org/10.1016/j.jhazmat.2015.09.060.

Gao, Y., Zong, J., Que, H., Zhou, Z., Xiao, M., Chen, S., 2017. Inoculation with arbuscular mycorrhizal fungi increases glomalin-related soil protein content and PAH removal in soils planted with Medicago sativa L. Soil Biol. Biochem. 115, 148–151. https://doi.org/10.1016/j.soilbio.2017.08.023.

Gerdemann, J., Nicolson, T.H., 1963. Spores of mycorrhizal Endogone species extracted from soil by wet sieving and decanting. Transac. Br. Mycol. Soc. 46, 235–244. https://doi.org/10.1016/S0007-1536(63)80079-0.

Gillespie, A.W., Farrell, R.E., Walley, F.L., Ross, A.R., Leinweber, P., Eckhardt, K.-U., Regier, T.Z., Blyth, R.I., 2011. Glomalin-related soil protein contains non-mycorrhizal-related heat-stable proteins, lipids and humic materials. Soil Biol. Biochem. 43, 766–777. https://doi.org/10.1016/j.soilbio.2010.12.010.

Giovannetti, M., Mosse, B., 1980. An evaluation of techniques for measuring vesicular arbuscular mycorrhizal infection in roots. New Phytol. 84, 489–500. https://www.jstor.org/stable/2432123.

Gonzalez-Chavez, M.C., Carrillo-Gonzalez, R., Wright, S.F., Nichols, K.A., 2004. The role of glomalin, a protein produced by arbuscular mycorrhizal fungi, in sequestering potentially toxic elements. Environ. Pollut. 130, 317–323. https://doi.org/10.1016/j.envpol.2004.01.004.

Harner, M.J., Ramsey, P.W., Rillig, M.C., 2004. Protein accumulation and distribution in floodplain soils and river foam. Ecol. Lett. 7, 829–836. https://doi.org/10.1111/j.1461-0248.2004.00638.x.

Johnston, C., Aochi, Y., 1996. Fourier transform infrared and Raman spectroscopy, Methods of Soil Analysis Part 3—Chemical Methods. pp. 269–321.

Kumar, S., Singh, A.K., Ghosh, P., 2018. Distribution of soil organic carbon and glomalin related soil protein in reclaimed coal mine-land chronosequence under tropical condition. Sci. Total Environ. 625, 1341–1350. https://doi.org/10.1016/j.scitotenv.2018.01.061.

Li, Q.S., Chen, Y., Fu, H.B., Cui, L., Shi, L., Wang, L.L., Liu, Z.F., 2012. Health risk of heavy metals in food crops grown on reclaimed tidal flat soil in the Pearl River Estuary, China. J. Hazard. Mater. 227, 148–154. https://doi.org/10.1016/j.jhazmat.2012.05.023.

Liu, J.L., Wu, H., Feng, J.X., Li, Z.J., Lin, G.H., 2014. Heavy metal contamination and ecological risk assessments in the sediments and zoobenthos of selected mangrove ecosystems, South China. Catena 119, 136–142. https://doi.org/10.1016/j.catena.2014.02.009.

López-Merino, L., Serrano, O., Adame, M.F., Mateo, M.Á., Cortizas, A.M., 2015. Glomalin accumulated in seagrass sediments reveals past alterations in soil quality due to land-use change. Global Planet. Change 133, 87–95. https://doi.org/10.1016/j.gloplacha.2015.08.004.

Lovelock, C.E., Wright, S.F., Clark, D.A., Ruess, R.W., 2004. Soil stocks of glomalin produced by arbuscular mycorrhizal fungi across a tropical rain forest landscape. J. Ecol. 92, 278–287. https://doi.org/10.1111/j.0022-0477.2004.00855.x.

Malekzadeh, E., Aliasgharzad, N., Majidi, J., Abdolalizadeh, J., Aghebati-Maleki, L., 2016. Contribution of glomalin to Pb sequestration by arbuscular mycorrhizal fungus in a sand culture system with clover plant. Eur. J. Soil Biol. 74, 45–51. https://doi.org/10.1016/j.ejsobi.2016.03.003.

Millero, F.J., Woosley, R., Ditrolio, B., Waters, J., 2009. Effect of ocean acidification on the speciation of metals in seawater. Oceanography 22, 72–85. https://www.jstor.org/stable/24861025.

Montazer-Rahmati, M.M., Rabbani, P., Abdolali, A., Keshtkar, A.R., 2011. Kinetics and equilibrium studies on biosorption of cadmium, lead, and nickel ions from aqueous solutions by intact and chemically modified brown algae. J. Hazard. Mater. 185, 401–407. https://doi.org/10.1016/j.jhazmat.2010.09.047.

Ozturk, S., Aslim, B., Suludere, Z., 2010. Cadmium (II) sequestration characteristics by two isolates of *Synechocystis* sp. in terms of exopolysaccharide (EPS) production and monomer composition. Bioresource Technol. 101, 9742–9748. https://doi.org/10.1016/j.biortech.2010.07.105.

Pace, M.L., Cole, J.J., Carpenter, S.R., Kitchell, J.F., Hodgson, J.R., Van de Bogert, M.C., Bade, D.L., Kritzberg, E.S., Bastviken, D., 2004. Whole-lake carbon-13 additions reveal terrestrial support of aquatic food webs. Nature 427, 240.

Rillig, M.C., 2004. Arbuscular mycorrhizae, glomalin, and soil aggregation. Can. J. Soil Sci. 84, 355–363. https://doi.org/10.4141/S04-003.

Rillig, M.C., Wright, S.F., Nichols, K.A., Schmidt, W.F., Torn, M.S., 2001. Large contribution of arbuscular mycorrhizal fungi to soil carbon pools in tropical forest soils. Plant Soil 233, 167–177. https://doi.org/10.1023/A:1010364221169.

Rillig, M.C., Caldwell, B.A., Wösten, H.A., Sollins, P., 2007. Role of proteins in soil carbon and nitrogen storage: controls on persistence. Biogeochemistry 85, 25–44. https://doi.org/10.1007/s10533-007-9102-6.

Schiff, K., Diehl, D., Valkirs, A., 2004. Copper emissions from antifouling paint on recreational vessels. Mar. Pollut. Bull. 48, 371–377. https://doi.org/10.1016/j.marpolbul.2003.08.016.

Schindler, F.V., Mercer, E.J., Rice, J.A., 2007. Chemical characteristics of glomalin-related soil protein (GRSP) extracted from soils of varying organic matter content. Soil Biol. Biochem. 39, 320–329. https://doi.org/10.1016/j.soilbio.2006.08.017.

Sheng, G.-P., Yu, H.-Q., Li, X.-Y., 2010. Extracellular polymeric substances (EPS) of microbial aggregates in biological wastewater treatment systems: a review. Biotechnol. Adv. 28, 882–894. https://doi.org/10.1016/j.biotechadv.2010.08.001.

Singh, A.K., Rai, A., Singh, N., 2016. Effect of long term land use systems on fractions of glomalin and soil organic carbon in the Indo-Gangetic plain. Geoderma 277, 41–50. https://doi.org/10.1016/j.geoderma.2016.05.004.

Singh, A.K., Rai, A., Pandey, V., Singh, N., 2017. Contribution of glomalin to dissolve organic carbon under different land uses and seasonality in dry tropics. J. Environ. Manage. 192, 142–149. https://doi.org/10.1016/j.jenvman.2017.01.041.

Smith, S.E., Read, D.J., 2010. Mycorrhizal Symbiosis. Academic Press.

Sun, P., Hui, C., Bai, N., Yang, S., Wan, L., Zhang, Q., Zhao, Y., 2015. Revealing the characteristics of a novel bioflocculant and its flocculation performance in *Microcystis aeruginosa* removal. Sci. Rep. 5, 17465. https://doi.org/10.1038/srep17465.

Vodnik, D., Grčman, H., Maček, I., Van Elteren, J., Kovačevič, M., 2008. The contribution of glomalin-related soil protein to Pb and Zn sequestration in polluted soil. Sci. Total Environ. 392, 130–136. https://doi.org/10.1016/j.scitotenv.2007.11.016.

Wang, Y., Qiu, Q., Yang, Z., Hu, Z., Tam, N.F.-Y., Xin, G., 2010. Arbuscular mycorrhizal fungi in two mangroves in South China. Plant Soil 331, 181–191. https://doi.org/10.1007/s11104-009-0244-2.

Wang, Q., Wu, Y., Wang, W., Zhong, Z., Pei, Z., Ren, J., Wang, H., Zu, Y., 2014. Spatial variations in concentration, compositions of glomalin related soil protein in poplar plantations in northeastern China, and possible relations with soil physicochemical properties. Sci. World J. 2014https://doi.org/10.1155/2014/160403. 160403.

Wang, Q., Wang, W., He, X., Zhang, W., Song, K., Han, S., 2015. Role and variation of the amount and composition of glomalin in soil properties in farmland and adjacent plantations with reference to a primary forest in North-Eastern China. PLoS One 10, e0139623. https://doi.org/10.1371/journal.pone.0139623.

Wang, Q., Lu, H., Chen, J., Hong, H., Liu, J., Li, J., Yan, C., 2018a. Spatial distribution of glomalin-related soil protein and its relationship with sediment carbon sequestration across a mangrove forest. Sci. Total Environ. 613-614, 548–556. https://doi.org/10.1016/j.scitotenv.2017.09.140.

Wang, Q., Li, J., Chen, J., Hong, H., Lu, H., Liu, J., Dong, Y., Yan, C., 2018b. Glomalin-related soil protein deposition and carbon sequestration in the Old Yellow River delta. Sci. Total Environ. 625, 619–626. https://doi.org/10.1016/j.scitotenv.2017.12.303.

Wang, Q., Mei, D.G., Chen, J.Y., Lin, Y.S., Liu, J.C., Lu, H.L., Yan, C.L., 2019. Sequestration of heavy metal by glomalin-related soil protein: Implication for water quality improvement in mangrove wetlands. Water Res. 148, 142–152. https://doi.org/10.1016/j.watres.2018.10.043.

Wright, S.F., Upadhyaya, A., 1996. Extraction of an abundant and unusual protein from soil and comparison with hyphal protein of arbuscular mycorrhizal fungi. Soil Sci. 161, 575–586.

Wright, S.F., Upadhyaya, A., 1998. A survey of soils for aggregate stability and glomalin, a glycoprotein produced by hyphae of arbuscular mycorrhizal fungi. Plant Soil 198, 97–107. https://doi.org/10.1023/A:1004347701584.

Xia, B., Sui, Q., Sun, X.M., Han, Q., Chen, B.J., Zhu, L., Qu, K.M., 2018. Ocean acidification increases the toxic effects of TiO2 nanoparticles on the marine microalga *Chlorella vulgaris*. J. Hazard. Mater. 346, 1–9. https://doi.org/10.1016/j.jhazmat.2017.12.017.

Xie, X., Weng, B., Cai, B., Dong, Y., Yan, C., 2014. Effects of arbuscular mycorrhizal inoculation and phosphorus supply on the growth and nutrient uptake of *Kandelia obovata* (Sheue, Liu & Yong) seedlings in autoclaved soil. Appl. Soil Ecol. 75, 162–171. https://doi.org/10.1016/j.apsoil.2013.11.009.

Yin, C., Meng, F., Chen, G.H., 2015. Spectroscopic characterization of extracellular polymeric substances from a mixed culture dominated by ammonia-oxidizing bacteria. Water Res. 68, 740–749. https://doi.org/10.1016/j.watres.2014.10.046.

Yuan, S.-J., Sun, M., Sheng, G.-P., Li, Y., Li, W.-W., Yao, R.-S., Yu, H.-Q., 2010. Identification of key constituents and structure of the extracellular polymeric substances excreted by *Bacillus megaterium* TF10 for their flocculation capacity. Environ. Sci. Technol. 45, 1152–1157. https://doi.org/10.1021/es1030905.

Yue, Z.-B., Li, Q., Li, C.-c., Chen, T.-h., Wang, J., 2015. Component analysis and heavy metal adsorption ability of extracellular polymeric substances (EPS) from sulfate reducing bacteria. Bioresource Technol. 194, 399–402. https://doi.org/10.1016/j.biortech.2015.07.042.

Zhang, Z.-W., Xu, X.-R., Sun, Y.-X., Yu, S., Chen, Y.-S., Peng, J.-X., 2014. Heavy metal and organic contaminants in mangrove ecosystems of China: a review. Environ. Sci. Pollut. Res. 21, 11938–11950. https://doi.org/10.1007/s11356-014-3100-8.

Zhang, J., Tang, X., He, X., Liu, J., 2015. Glomalin-related soil protein responses to elevated CO2 and nitrogen addition in a subtropical forest: Potential consequences for soil carbon accumulation. Soil Biol. Biochem. 83, 142–149. https://doi.org/10.1016/j.soilbio.2015.01.023.

Zhang, J., Tang, X., Zhong, S., Yin, G., Gao, Y., He, X., 2017a. Recalcitrant carbon components in glomalin-related soil protein facilitate soil organic carbon preservation in tropical forests. Sci. Rep. 7, 2391. https://doi.org/10.1038/s41598-017-02486-6.

Zhang, Z., Wang, Q., Wang, H., Nie, S., Liang, Z., 2017b. Effects of soil salinity on the content, composition, and ion binding capacity of glomalin-related soil protein (GRSP). Sci. Total Environ. 581-582, 657–665. https://doi.org/10.1016/j.scitotenv.2016.12.176.